Available online at www.sciencedirect.com
ScienceDirect
Trans. Nonferrous Met. Soc. China 23(2013) 3604−3610
Transactions of Nonferrous Metals Society of China
www.tnmsc.cn

Microstructure and mechanical properties of as-cast Mg−Sn−Ca alloys and effect of alloying elements

K. SURESH[1], K.P. RAO[1], Y.V.R.K. PRASAD[2], N. HORT[3], K.U. KAINER[3]

1. Department of Mechanical and Biomedical Engineering, City University of Hong Kong, Kowloon, Hong Kong, China;
2. Consultant, processingmaps.com, No. 2/B, Vinayaka Nagar, Hebbal, Bengaluru 560024, India;
3. Helmholtz-Zentrum Geesthacht, Institute of Materials Research, Magnesium Innovation Centre, Max-Planck-Straße 1, Geesthacht 21502, Germany

Received 27 March 2013; accepted 18 June 2013

Abstract: The effect of Sn, Ca, Al, Si and Zn addition on the compressive strength of cast Mg−Sn−Ca (TX) alloys was studied in the temperature range of 25−250 °C and correlated with the microstructure. The Sn to Ca mass ratio up to 2.5 contributes to the formation of Mg_2Ca phase at the grain boundaries and CaMgSn in the matrix, while a ratio of 3 gives only CaMgSn phase mostly in the matrix. While the compressive strength decreases with the increase in temperature, for Sn/Ca up to 2.5, a plateau occurs in 100−175 °C, which is attributed to the strengthening by Mg_2Ca. However, for ratio of 3, the strength is lower and decreases more gradually. Mg−3Sn−2Ca (TX32) has the highest strength and the addition of 0.4% Al increases its strength but simultaneous addition of Si lowers the strength. Likewise, the addition of Zn improves its strength but simultaneous addition of Al slightly decreases the strength. The results are correlated with the types of intermetallic phases that form in various alloys.
Key words: Sn/Ca ratio; Mg−Sn−Ca alloys; alloying additions; microstructure, compressive strength

1 Introduction

In view of their low density, high specific strength and damping capacity, magnesium alloys are being developed for applications in automotive, aerospace, electronics and sporting goods industries. In general, AZ and AM series of wrought Mg alloys are being investigated due to theirs good mechanical properties although they have problems associated with lower creep and corrosion resistance [1−3]. To mitigate some of these problems, an alternate alloy system based on Mg−Sn−Ca (TX series) is being considered [4]. Sn has a low melting point while Ca has a low density. In Mg−Sn−Ca system, Sn forms a solid solution with Mg and imparts corrosion resistance whereas Ca forms thermally stable intermetallic particles in the matrix to enhance creep strength [5,6]. It is observed that the alloy with Sn/Ca ratio of 1.5 provides the lowest creep rate [6] since Mg_2Ca formed at the grain boundaries reduces grain boundary sliding. However, the alloy with higher Sn/Ca ratio of 5 (Mg−5Sn−1Ca) forms Mg_2Sn phase which is thermally sensitive and lowers the creep resistance [5]. So the ratio of Sn/Ca is an important variable in deciding the properties of this ternary alloy and TX32 is a suitable choice in view of its acceptable creep properties. The alloying addition of Al and Zn may be considered to further strengthen this ternary alloy as they form solid solution with Mg and cause strengthening. The addition of Si promotes the formation of intermetallic compounds such as CaMgSi and Mg_2Si [7] that would adversely affect the tensile properties while creep properties may be improved [8].

There are two objectives in this investigation. The first one is to examine the effect of Sn/Ca ratio on the higher temperature compressive strength of ternary Mg−Sn−Ca alloys and establish a correlation with the phase constituents present in the microstructure. Two sets of alloys are chosen for this purpose. 1) The Sn/Ca mass ratio is increased by increasing Sn content and keeping Ca constant. 2) Both Sn and Ca contents are changed while keeping Sn/Ca ratio constant at 3. The second objective is to evaluate the effect of other ternary and quaternary additions on the strength of TX32 alloy. For

Corresponding author: K.P. RAO; Tel: +852-3442-8409; Fax: +852-3442-0172; E-mail: mekprao@cityu.edu.hk
DOI: 10.1016/S1003-6326(13)62907-6

this purpose, further additions of Al, Al+Si, Zn or Al+Zn are made to TX32 alloy and the resultant mechanical properties are evaluated.

2 Experimental

The nominal compositions of the alloys studied are given in Table 1. The alloys were melted under a protective cover of Ar+3%SF_6 mixed gas atmosphere and poured in pre-heated permanent molds at a temperature of about 720 °C to produce cylindrical billets of 100 mm in diameter and 350 mm in height. Cylindrical specimens of 10 mm in diameter and 15 mm in height for compression testing were machined from the cast billets. For evaluating the compressive strength, slow strain rate or static compression tests were conducted at different temperatures in the range of 25−250 °C and at a strain rate of 0.0001 s^{-1} using a computer-controlled servo-hydraulic testing machine (DARTEC, UK, M1000/RK). The temperature during the test was measured using a thermocouple embedded in a 1 mm diameter and 5 mm depth hole drilled at mid-height to the centre of the specimen. Graphite powder mixed with grease was used as the lubricant. Using standard equations, the load−stroke data were converted into true stress−true strain curves and the ultimate compressive strength was recorded.

The microstructural features of the alloys were characterized using optical metallurgical microscope (OMM – OLYMPUS/PMG3) and scanning electron microscope (SEM−JEOL JSM-5600) equipped with energy dispersive spectroscope (EDS−OXFORD/AZtec). The X-ray diffraction (XRD) was conducted using the Siemens D-5000 diffractometer with Cu K_α radiation (λ=1.5406 Å) in the 2θ range between 20° and 80° with the scanning step of 0.05°. The main constituent phases of the alloys were confirmed using XRD and EDS mapping. Micro-hardness in HV was measured using a load of 500 mN (MH−Fischerscope HM2000 XYp).

3 Results and discussion

3.1 Effect of Sn/Ca ratio

3.1.1 As-cast microstructure

The initial microstructures of as-cast TX22 are shown in Fig. 1 which is typical of all other alloys, except TX62 in the first set. The microstructure exhibits two phases with a large volume of Mg_2Ca phase at the grain boundaries and needle-like CaMgSn intermetallic particles within the matrix. Mg_2Ca phase is present to a small extent in TX52. The microstructure of TX62 is shown in Fig. 2, which is typical of the alloys in the second set including TX41 and TX31. The microstructure exhibits only the ternary phase CaMgSn and it appears that a Sn/Ca mass ratio of 3 binds nearly all the Ca in forming CaMgSn particles while the

Table 1 Selected as-cast magnesium alloys with their nominal composition, main intermetallic phases present, grain size and hardness

Composition (mass fraction, %)	Designation	Main phase	Typical grain size/μm	Micro-hardness range (HV)
Mg−2Sn−2Ca	TX22	Mg_2Ca, CaMgSn	350	38−43
Mg−3Sn−2Ca	TX32	Mg_2Ca, CaMgSn	455	40−48
Mg−4Sn−2Ca	TX42	Mg_2Ca, CaMgSn	570	46−55
Mg−5Sn−2Ca	TX52	CaMgSn, Mg_2Ca (small)	500	47−56
Mg−3Sn−1Ca	TX31	CaMgSn	>500	38−48
Mg−4.5Sn−1.5Ca	TX41	CaMgSn	>500	37−46
Mg−6Sn−2Ca	TX62	CaMgSn	>800	37−48
Mg−3Sn−2Ca−0.4Al	TXA320	$(Mg,Al)_2Ca$, Ca_2Sn_Mg	250	48−52
Mg−3Sn−2Ca−1Al	TXA321	$(Mg,Al)_2Ca$, Ca_2Sn_Mg	300	45−52
Mg−3Sn−2Ca−0.4Al−0.2Si	TXA320−S.02	Ca_2Sn_Mg, CaMgSi, Mg_2Ca	600	42−52
Mg−3Sn−2Ca−0.4Al−0.4Si	TXA320−S.04	Ca_2Sn_Mg, CaMgSi, Mg_2Ca (small)	500	47−59
Mg−3Sn−2Ca−0.4Al−0.6Si	TXA320−S.06	Ca_2Sn_Mg, CaMgSi	550	40−54
Mg−3Sn−2Ca−0.4Al−0.8Si	TXA320−S.08	Ca_2Sn_Mg, CaMgSi	800	48−52
Mg−3Sn−2Ca−0.4Zn	TXZ320	Mg_2Ca, Ca_2Sn_Mg, $Ca_2Mg_6Zn_3$	230	49−60
Mg−3Sn−2Ca−1Zn	TXZ321	Mg_2Ca, Ca_2Sn_Mg, $Ca_2Mg_6Zn_3$	220	58−63
Mg−3Sn−2Ca−0.4Al−0.4Zn	TXAZ3200	$(Mg,Al)_2Ca$, Ca_2Sn_Mg, $Ca_2Mg_6Zn_3$	140	49−64
Mg−3Sn−2Ca−1Al−1Zn	TXAZ3211	$(Mg,Al)_2Ca$, Ca_2Sn_Mg, $Ca_2Mg_6Zn_3$	135	47−61

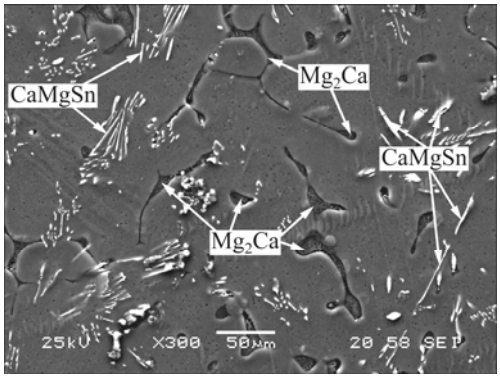

Fig. 1 SEM image of as-cast TX22 (Mg−2Sn−2Ca) alloy

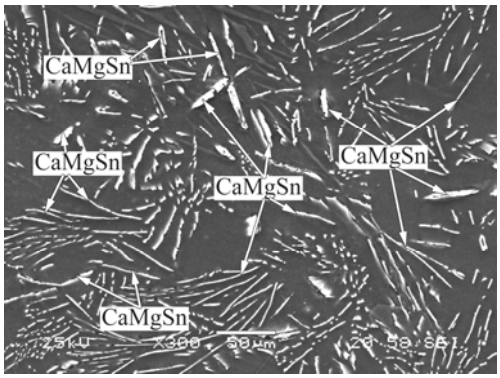

Fig. 2 SEM image of as-cast TX62 (Mg−6Sn−2Ca) alloy

remaining Sn dissolves in the matrix. The average grain diameter is very large (350−800 μm) in all the cases and the micro-hardness values vary in the range of HV 38−56 (Table 1). The existence of these two phases in the alloys with different Sn/Ca ratios has been reported [6,9−13].

3.1.2 Compressive behavior

The typical true stress−true strain curves obtained on TX32 alloy at different temperatures are shown in Fig. 3. The other alloys with different Sn/Ca ratio also exhibit similar stress−strain behavior. All alloys exhibit good ductility at 250 °C indicating the beginning of workability temperature range.

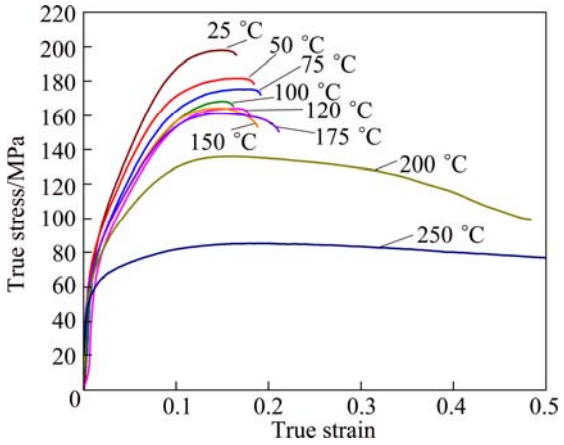

Fig. 3 Compressive true stress−true strain curves of as-cast TX32 alloy at various temperatures

The photographs of the specimens compressed at different temperatures are shown in Fig. 4. All the specimens deformed at temperatures less than 150 °C exhibit shear fracture caused by adiabatic shear bands which are formed at about 45° with respect to the compression axis. At higher temperatures, the deformation is characterized by shear localization where the localized bands are formed at about 35° with respect to the compression axis. In view of limited slip systems in the alloys (mostly basal slip) and strengthening by CaMgSn precipitates in the matrix, all the alloys exhibit low ductility due to flow localization at temperatures less than 200 °C. At temperature higher than 225 °C, prismatic slip occurs in addition to basal slip and thus enhances the ductility.

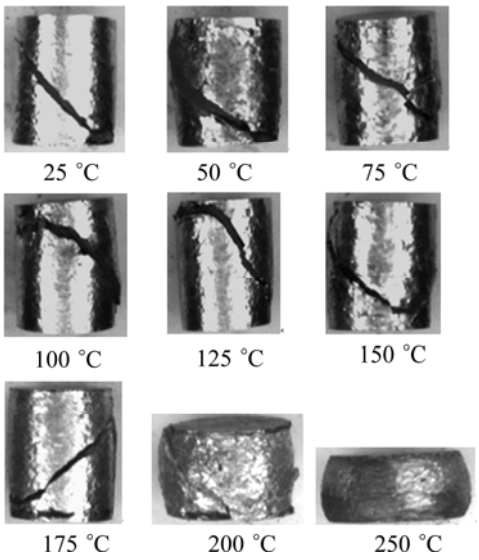

Fig. 4 Photographs of specimens of as-cast TX42 (Mg−4Sn−2Ca) compressed at different temperatures between 25−250 °C and strain rate of 0.0001 s^{-1} (the compression axis is vertical)

3.1.3 Compressive strength

The variation of ultimate compressive strength (UCS) of Mg−Sn−Ca alloys having different Sn/Ca ratios with temperature is shown in Fig. 5. The compressive strength of all Mg−Sn−Ca alloys is shown as a function of temperature in Fig. 6. The error estimated for the data is within 5%. At each temperature, the strength is nearly unaffected by Sn/Ca ratio from 1 to 2.5, but dropped for the ratio of 3 (TX62). It may be recalled that all the alloys with Sn/Ca ratio up to 2.5 have Mg_2Ca phase at the grain boundaries and this strengthens them and reduces their sliding. On the other hand, when the Sn/Ca ratio is 3, only CaMgSn particles are present in the matrix, and the grain boundary sliding reduces the strength with increasing temperature. Thus, Mg_2Ca phase at the grain boundaries is beneficial in

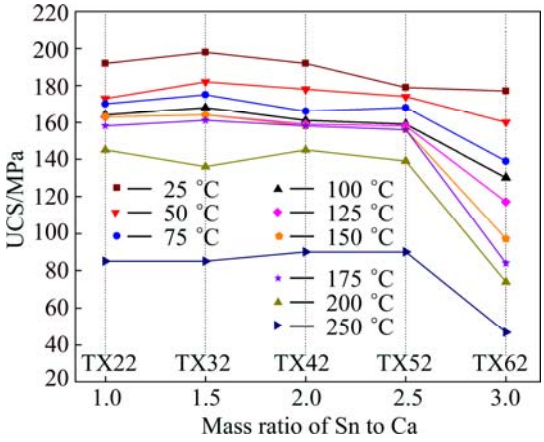

Fig. 5 Variation of ultimate compressive strength of as-cast Mg−Sn−Ca alloys with different Sn to Ca mass ratios

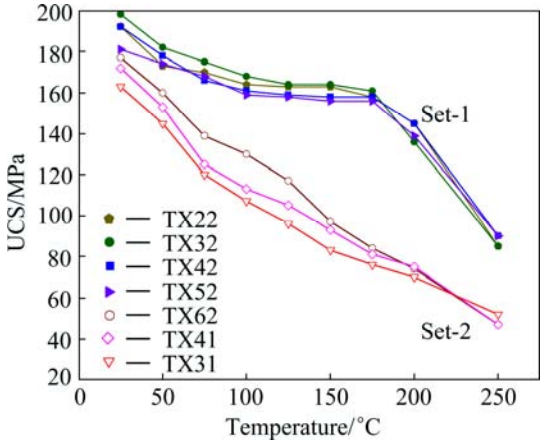

Fig. 6 Variation of ultimate compressive strength of as-cast Mg−Sn−Ca alloys with temperature

retaining the strength over a temperature range of 25−175 °C.

The behavior is different for the two sets of alloys as shown in Fig. 6. In the first set of alloys (TX22, TX32, TX42 and TX52) where the Sn/Ca ratio is less than 3, the strength decreases with temperature up to about 100 °C, and reaches a near plateau before rapidly falling beyond 175 °C. The microstructures of these alloys show that CaMgSn phase is present in the matrix and Mg_2Ca phase is at grain boundaries. The Mg_2Ca phase strengthens the grain boundaries and reduces their sliding due to pinning which may be responsible for the occurrence of plateau in the strength variation. At temperature higher than 175 °C, thermal energy overcomes the pinning effect and grain boundary sliding resumes. The strength of as-cast TX32 at temperatures of 25−175 °C is the highest among all the Mg−Sn−Ca alloys studied.

In the second set of alloys (TX62, TX41 and TX31 with Sn/Ca ratio of 3), the strength (UCS) continuously decreases with temperature. These alloys are strengthened by CaMgSn precipitates and are relatively free from grain boundary precipitates. However, this intermetallic phase does not play a significant role in enhancing the mechanical properties [14]. TX62 is stronger than TX41 and TX31 because of the higher volume of CaMgSn.

3.2 TX32 alloy with Al and Al+Si additions

3.2.1 As-cast microstructure

The intermetallic phases identified in TX32+Al and TX32+Al+Si alloys are given in Table 1. The microstructure of the starting material of as-cast TXA320−S0.4 (Mg−3Sn−2Ca−0.4Al−0.4Si) alloy is shown in Fig. 7. In this quaternary alloy, Ca_2Sn_Mg and CaMgSi phases are present in the matrix whereas a small amount of Mg_2Ca is present at the grain boundaries. That is, a small amount of Si addition develops an entirely different set of intermetallic phases (Ca_2Sn and CaMgSi) instead of CaMgSn phase in the base alloy TX32 [7].

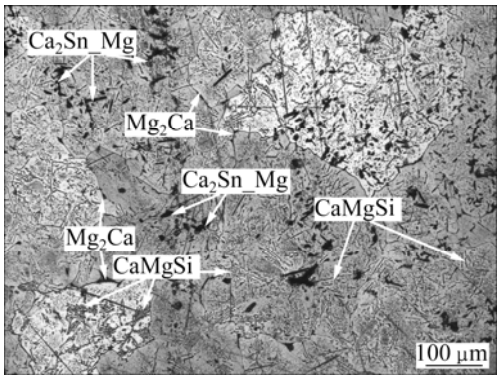

Fig. 7 Optical microstructure of as-cast TXA320−S0.4 alloy

3.2.2 Compressive strength

The variation of UCS of as-cast Mg−3Sn−2Ca−0.4Al alloy (TXA320) with increased additions of Si (0.2%−0.8%, in step of 0.2%) as a function of temperature (25−250 °C) is shown in Fig. 8 along with the base alloy TX32. The alloy TX32 with 0.4% Al shows compressive strength that is slightly higher than that of TX32 based alloy up to temperature 100 °C. The addition of Si to TXA320 results in a reduction in strength, in particular with increase in temperature. The addition of Si often promotes the precipitation of Si containing particles, such as CaMgSi, which form during solidification and are quite detrimental to the mechanical properties of Mg alloys [15,16]. The strength drops gradually with increasing temperature and reaches a near plateau between 100 °C to 175 °C beyond which it drops rapidly. The formation of other compounds containing Al and Si can be discounted due to negligible solid solubility of Si in Mg [17]. It has been observed that ultimate tensile strength (UTS) decreases with increasing Si content [18] in cast Mg−Al−Si composites. Also, the addition of Si to some aluminum containing magnesium

alloys improves creep resistance while reducing the tensile properties [8]. The present results clearly show that, unlike the Al addition, Si addition is not useful for improving the strength of the base alloy TX32.

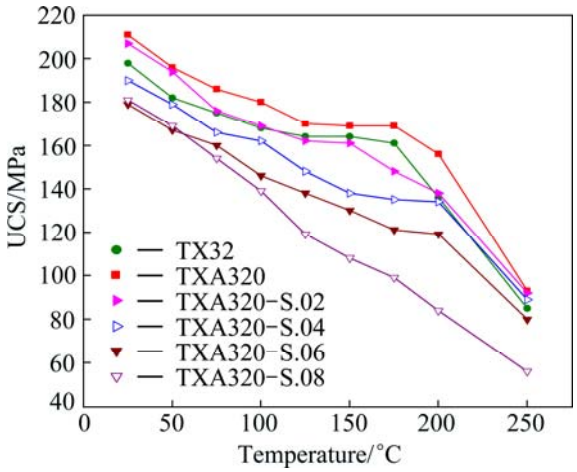

Fig. 8 Variation of ultimate compressive strength of as-cast Mg−3Sn−2Ca with addition of Al and Al+Si with temperature

3.3 TX32 alloy with addition of Al, Zn and Al+Zn

3.3.1 As-cast microstructure

The microstructures of as-cast TXA321 and TXZ321 alloys are shown in Figs. 9 and 10. The phases identified in these alloys are given in Table 1. Ca_2Sn_Mg, Mg_2Ca and $Ca_2Mg_6Zn_3$ are present in the quaternary TX32+Zn alloys. The existence of the above phases was confirmed by X-ray diffractometry and is shown in Fig. 11(a). The possible formation of $Ca_2Mg_6Zn_3$ phase by the addition of Zn to TX32 based alloy is also indicated by EDS shown in Fig. 11(b), and the phase is similar to that reported on Mg−Ca−Zn alloy system [19−23]. Al addition facilitates the formation of Ca_2Sn_Mg, Mg_2Ca and Al_2Ca or $(Mg,Al)_2Ca$. The grain size reduces significantly due to the addition of Al, Zn, or both, the latter being most significant.

3.3.2 Compressive strength

The high-temperature compressive strength values of TX32 alloy containing Al, Zn or Al+Zn with temperature in the range of 25−250 °C are shown in Fig. 12. The strength decreases initially with temperature from 25 to 100 °C and reaches a near plateau in the range of 100−175 °C beyond which it drops sharply. In alloys with grain boundary phases, the occurrence of plateau may be attributed to the presence of intermetallic particles at the grain boundaries which act as barriers to the dislocation motion and grain boundary sliding. The barriers can be overcome if the thermal energy is sufficient to cross the obstacles at higher temperatures and hence, strength drops from 200 °C.

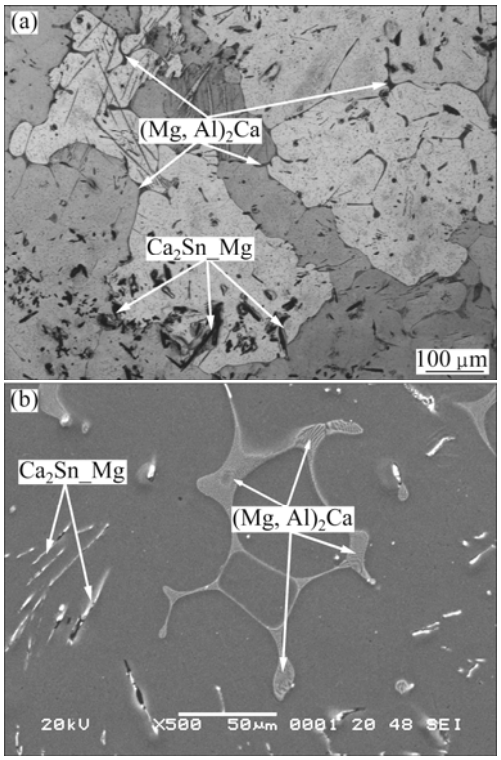

Fig. 9 Microstructures of as-cast TXA321 alloy: (a) Optical image; (b) SEM image

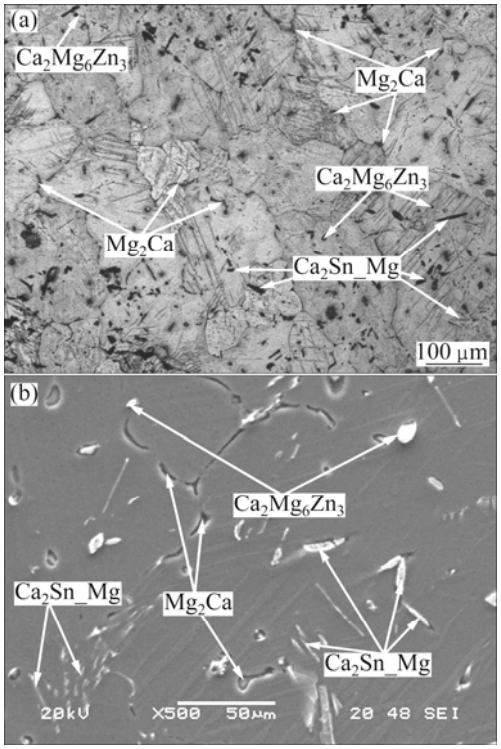

Fig. 10 Microstructures of as-cast TXZ321 alloy: (a) Optical image; (b) SEM image

The alloys with either Al or Zn show significantly increased strength compared to their TX32 based alloy at most of the test temperatures. The alloy with 1% Zn

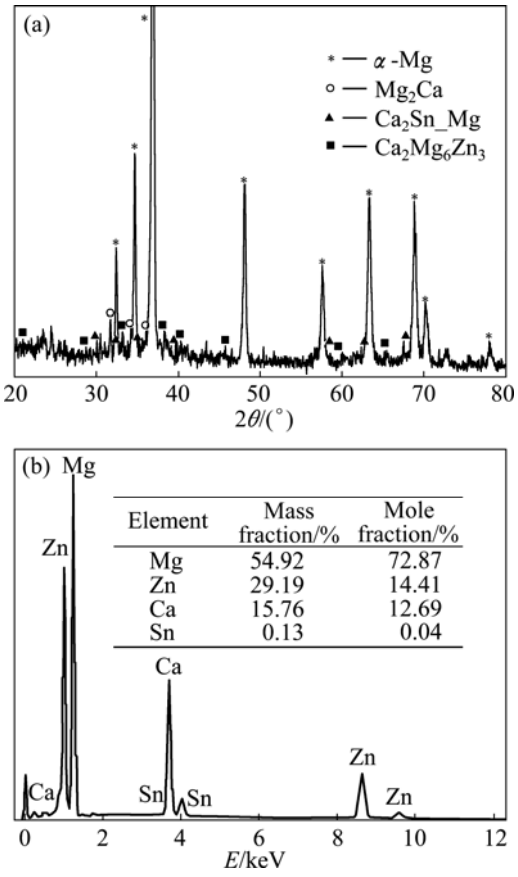

Element	Mass fraction/%	Mole fraction/%
Mg	54.92	72.87
Zn	29.19	14.41
Ca	15.76	12.69
Sn	0.13	0.04

Fig. 11 XRD pattern (a) and EDS spectrum (b) of as-cast TXZ321 alloy

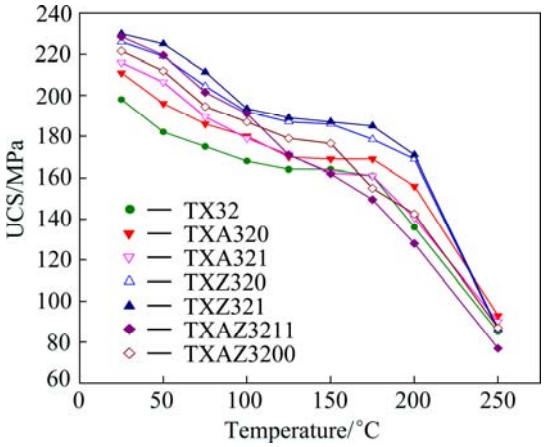

Fig. 12 Variation of ultimate compressive strength of as-cast Mg−3Sn−2Ca with addition of Al, Zn and Al+Zn with temperature

addition exhibits the highest compressive strength among these alloys, which shows that solid solution strengthening by Zn is significant. Also, contribution due to the precipitation of intermetallic phase $Ca_2Mg_6Zn_3$ will also be additive [19,20]. The alloys with the addition of Al+Zn together show intermediate levels of strength, indicating the strengthening effect of these two elements in magnesium alloys [24,25].

4 Conclusions

1) In ternary alloys with Sn/Ca mass ratio up to 2.5, the microstructure consists of CaMgSn phase in the matrix and Mg_2Ca phase at grain boundaries, while in alloys with the mass ratio of 3 only CaMgSn phase is present.

2) In alloys with Sn/Ca mass ratio up to 2.5, the variation of compressive strength with temperature exhibits a plateau in the temperature range of 100−175 °C, which may be attributed to the presence of Mg_2Ca phase at the grain boundaries.

3) When the Sn/Ca mass ratio is 3, the compressive strength is lower than that with a mass ratio less than 2.5 and decreases more rapidly with increase in temperature.

4) The strength of as-cast TX32 is the highest among all the ternary Mg−Sn−Ca alloys studied.

5) The addition of Zn to TX32 significantly improves the strength compared with the addition of Al, while Si addition is detrimental.

Acknowledgement

The work presented in this paper has been fully supported by General Research Funds (Projects #115108 and #114809) from the Research Grants Council of the Hong Kong SAR, China. The authors would like to thank Mr. Yuen Chi HUNG for his assistance in conducting the compression tests.

References

[1] GHALI E, DIETZEL W, KAINER K U. General and localized corrosion of magnesium alloys: A critical review [J]. Journal of Materials Engineering and Performance, 2004, 13: 7−23.

[2] YUAN Quan, CHEN Bin, LUO Ji, ZHANG Ding-fei, QUAN Guo-zheng. Effect of temperature and heating rate on mechanical properties of magnesium alloy AZ31 [J]. Transactions of Nonferrous Metals Society of China, 2010, 20: s246−s249.

[3] SU Gui-hua, ZHANG Liang, CHENG Li-ren, LIU Yong-bing, CAO Zhan-yi. Microstructure and mechanical properties of Mg−6Al−0.3Mn−*x*Y alloys prepared by casting and hot rolling [J]. Transactions of Nonferrous Metals Society of China, 2010, 20: 383−389.

[4] ABU LEIL T, RAO K P, HORT N, KAINER K U. Corrosion behavior and microstructure of a broad range of Mg−Sn−X alloys [C]//Magnesium Technology 2006. Warrendale, PA: TMS, 2006: 281−286.

[5] ABU LEIL T, HORT N, DIETZEL W, BLAWERT C, HUANG Y, KAINER K U, RAO K P. Microstructure and corrosion behavior of Mg−Sn−Ca alloys after extrusion [J]. Transactions of Nonferrous Metals Society of China, 2009, 19: 40−44.

[6] HORT N, HUANG Y D, ABU LEIL T, RAO K P, KAINER K U. Properties and processing of magnesium−tin−calcium alloys [J]. Kovove Materialy, 2011, 49: 163−177.

[7] KOZLOV A, GROBNER J, SCHMID-FETZER R. Phase formation in Mg–Sn–Si and Mg–Sn–Si–Ca alloys [J]. Journal of Alloys and Compounds. 2011, 509: 3326−3337.

[8] ASL K M, TARI A, KHOMAMIZADEH F. The effect of different content of Al, RE and Si element on the microstructure, mechanical and creep properties of Mg−Al alloys [J]. Material Science and Engineering A, 2009, 523: 1−6.

[9] ARROYAVE R, LIU Z K. Intermetallics in the Mg−Ca−Sn ternary system: Structural, vibrational, and thermodynamic properties from first principles [J]. Physical Review B, 2006, 74: 174118.

[10] KOZLOV A, OHNO M, ARROYAVE R, LIU Z K, SCHMID-FETZER R. Phase equilibria, thermodynamics and solidification microstructures of Mg−Sn−Ca alloys. Part 1: Experimental investigation and thermodynamic modeling of the ternary Mg−Sn−Ca system [J]. Intermetallics, 2008, 16: 299−315.

[11] KOZLOV A, OHNO M, ABU LEIL T, HORT N, KAINER K U, SCHMID-FETZER R. Phase equilibria, thermodynamics and solidification microstructures of Mg−Sn−Ca alloys. Part 2: Prediction of phase formation in Mg-rich Mg−Sn−Ca cast alloys [J]. Intermetallics, 2008, 16: 316−321.

[12] ZHANG C, CAO H, FIROUZDOR V, KOU S, AUSTIN CHANG Y. Microstructure investigations of directionally solidified Mg-rich alloys containing Al, Ca and Sn [J]. Intermetallics, 2010, 18: 1597−1602.

[13] NAYYERI G, MAHMUDI R. The microstructure and impression creep behavior of cast, Mg−5Sn−*x*Ca alloys [J]. Materials Science and Engineering A, 2010, 527: 2087−2098.

[14] KIM D H, LEE J Y, LIM H K, KYEONG J S, KIM W T, KIM D H. The effect of microstructure evolution on the elevated temperature mechanical properties in Mg−Sn−Ca System [J]. Materials Transactions, 2008, 49: 2405−2413.

[15] KANG D H, PARK S S, KIM N J. Development of creep resistant die cast Mg–Sn–Al–Si alloy [J]. Materials Science and Engineering A, 2005, 413−414: 555−560.

[16] DARGUSCH M S, BOWLES A L, PETTERSEN K, BAKKE P, DUNLOP G L. The effect of silicon content on the microstructure and creep behavior in die-cast magnesium AS alloys [J]. Metallurgical and Materials Transactions A, 2004, 35: 1905−1909.

[17] SRINIVASAN A, PILLAI U T S, PAI B C. Microstructure and mechanical properties of Si and Sb added AZ91 magnesium alloy [J]. Metallurgical and Materials Transactions A, 2005, 36: 2235−2243.

[18] NANJUNDA SWAMY H M, NATH S K, RAY S. Tensile and fracture properties of cast and forged composite synthesized by addition of Al−Si alloy to magnesium [J]. Metallurgical and Materials Transactions A, 2009, 40: 3284−3293.

[19] LARIONOVA T V, PARK W W, YOU B S. A ternary phase observed in rapidly solidified Mg−Ca−Zn alloys [J]. Scripta Materialia, 2001, 45: 7−12.

[20] WASIUR-RAHMAN S, MEDRAJ M. Critical assessment and thermodynamic modeling of the binary Mg−Zn, Ca−Zn and ternary Mg−Ca−Zn systems [J]. Intermetallics, 2009, 17: 847−864.

[21] FINKEL A, SHEPELEVA L, BAMBERGER M, RABKIN E. The effect of exposure to elevated temperatures on the microstructure and hardness of Mg−Ca−Zn alloy alloys [C]// Magnesium Technology 2002. Warrendale, PA: TMS, 2002: 81−86.

[22] LEVI G, AVRAHAM S, ZILBEROV A, BAMBERGER M. Solidification, solution treatment and age hardening of a Mg−1.6wt% Ca−3.2wt% Zn alloy [J]. Acta Materialia, 2006, 54: 523−530.

[23] ZHOU Hong, WANG Yong, LIAO Zhi-dong. Microstructure and corrosion mechanism of as-cast Mg−Zn−Mn−Ca in Hank's solution [J]. Journal of Chongqing University, 2010, 9: 146−150.

[24] XIAO W, EASTON M A, ZHU S, DARGUSCH M S, GIBSON M A, JIA S, NIE J. Casting defects and mechanical properties of high pressure die cast Mg−Zn−Al−RE alloys [J]. Advanced Engineering Materials, 2012, 14: 68−76.

[25] ZHANG Jing, LI Zhong-sheng, GUO Zheng-xiao, PAN Fu-sheng. Solidification microstructural constituent and its crystallographic morphology of permanent-mould-cast Mg−Zn−Al alloys [J]. Transactions of Nonferrous Metals Society of China, 2006, 16: 452−458.

添加合金化元素对铸态 Mg−Sn−Ca 合金的显微组织和力学性能的影响

K. SURESH[1], K.P. RAO[1], Y.V.R.K. PRASAD[2], N. HORT[3], K.U. KAINER[3]

1. Department of Mechanical and Biomedical Engineering, City University of Hong Kong, Kowloon, Hong Kong, China;
2. Consultant, processingmaps.com, No. 2/B, Vinayaka Nagar, Hebbal, Bengaluru 560024, India;
3. Helmholtz-Zentrum Geesthacht, Institute of Materials Research, Magnesium Innovation Centre, Max-Planck-Straße 1, Geesthacht 21502, Germany

摘　要：在铸态 Mg−Sn−Ca (TX 系列)合金中添加不同含量的 Sn、Ca、Al、Si 和 Zn 等合金化元素，研究其在 25~250 °C 温度范围内的压缩强度和显微组织变化。当合金中 Sn/Ca 质量比到达 2.5 时，在晶界处有 Mg_2Ca 相生成；而当 Sn/Ca 质量比为 3 时，合金基体中只有 CaMgSn 相存在。当 Sn/Ca 质量比在 2.5 以上时，合金的压缩强度随着温度的升高而降低，在 100~1750 °C 保持基本不变，这主要是由于生成的 Mg_2Ca 相的强化作用所致。然而，当 Sn/Ca 质量比为 3 时，合金的强度较低，且随着温度的升高而下降更快。在这些合金中，Mg−3Sn−2Ca 合金的强度最高。向其中添加 0.4%Al 会导致其强度增加，然而同时添加 Si 会导致强度下降。同样地，添加 Zn 也能够提高合金的强度，而同时添加 Al 会导致强度下降。导致合金强度变化的原因与合金中生成的各种金属间化合物有关。

关键词：Sn/Ca 质量比；Mg−Sn−Ca 合金;合金化元素；显微组织；压缩强度

(Edited by Sai-qian YUAN)